THE JOURNAL OF PHYSICAL CHEMISTRY C

Article

pubs.acs.org/JPCC

Computational Study of Propylene and Propane Binding in Metal−Organic Frameworks Containing Highly Exposed Cu^+ or Ag^+ Cations

Ki Chul Kim,[†] Chang Yeon Lee,[‡,§] David Fairen-Jimenez,[∥] SonBinh T. Nguyen,[‡] Joseph T. Hupp,[‡] and Randall Q. Snurr*,[†]

[†]Department of Chemical and Biological Engineering, Northwestern University, 2145 Sheridan Rd., Evanston, Illinois 60208, United States

[‡]Department of Chemistry, Northwestern University, 2145 Sheridan Rd., Evanston, Illinois 60208, United States

[§]Department of Energy and Chemical Engineering, Incheon National University, Incheon 406-772, Republic of Korea

[∥]Department of Chemical Engineering and Biotechnology, University of Cambridge, Pembroke St., Cambridge CB2 3RA, U.K.

ABSTRACT: A synthetic route to create highly exposed, monovalent metal cations within the linkers of metal−organic frameworks (MOFs) is proposed and analyzed computationally. Quantum chemical calculations demonstrate the thermodynamic feasibility of incorporating Cu^+ or Ag^+ into a MOF containing an acetylene-bearing linker via postsynthesis modification. These highly exposed metal sites are predicted to bind propylene much more strongly than propane, suggesting their utility in adsorption separations. The nature of the propylene/metal binding is analyzed, and potential difficulties in activating the metal sites are discussed.

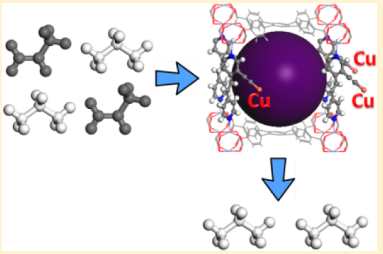

1. INTRODUCTION

Metal−organic frameworks (MOFs) are a family of nanoporous crystalline materials composed of metal ions or metal clusters linked by organic ligands, resulting in tailored nanoporous materials with outstanding surface areas.[1] The major advantage of MOFs over more conventional porous materials is the greater scope for tailoring these materials for specific applications. Because of their versatility, MOFs have attracted great interest in recent years for many applications including gas storage,[2−9] gas separation,[10−22] catalysis,[23−26] and chemical sensing.[27−32] In particular, gas separations (e.g., CO_2/CH_4,[12−16] CO_2/N_2,[17,18] and CO_2/H_2[19]) have received extensive interest due to the possibility of creating MOFs with specific adsorption sites, which are able to interact with particular molecules in a mixture.

One of the most challenging problems in the field of separations is the separation of propane/propylene mixtures. Propylene is an important commodity chemical, and its production requires it to be separated from propane on large scales. However, this separation presents considerable difficulties due to the similar physicochemical properties of propylene and propane. A number of researchers have investigated MOFs for propane/propylene separations recently.[33−46] In one of the earliest studies, Lamia et al. performed a combined simulation and experimental investigation of propylene and propane adsorption in HKUST-1.[33] They observed that, compared to propane, propylene exhibited relatively strong interaction with HKUST-1 due to specific interactions between the propylene π orbitals and the coordinatively unsaturated Cu sites of the MOF. Yoon et al. investigated the adsorption of propylene and propane in MIL-100(Fe), a MOF with coordinatively unsaturated Fe^{II} and Fe^{III} sites.[35] They reported that the exceptionally strong binding between propylene and MIL-100(Fe) results from the combination of (i) electron donation from the filled π orbital of propylene to a partially occupied d orbital of the coordinatively unsaturated Fe^{II} site and (ii) electron back-donation from the d orbital of the Fe^{II} site to the π^* antibonding orbital of propylene. Several groups have reported selective adsorption of propylene over propane in MOF-74, which also has open metal sites.[43−46]

These results suggest that selective adsorption of propylene in MOFs with open metal sites results from specific interactions between the π orbital of the propylene C−C double bond and an empty or partially occupied d orbital of the open transition metal sites. In all of the cases reported to date, the metal ions were part of the structural "nodes" of the MOF and exposed a single coordination site. We hypothesized that if more highly exposed metal sites could be created, they might exhibit interesting—and potentially even better—propane/propylene separation behavior. In this paper, we propose a postsynthesis procedure to incorporate open metal sites into MOF linkers. Our starting point is the DTO MOF reported by Lee et al.[37] As shown in Figure 1, DTO MOF is a noncatenated, pillared, paddlewheel MOF consisting of Zn^{2+} nodes coordinately linked by 1,2,4,5-tetrakis(carboxyphenyl)benzene (TCPB) and the dipyridyl strut L1, which contains an acetylene group (Figure 1).

Received: March 1, 2014
Revised: April 8, 2014
Published: April 11, 2014

ACS Publications © 2014 American Chemical Society

dx.doi.org/10.1021/jp502137j | J. Phys. Chem. C 2014, 118, 9086−9092

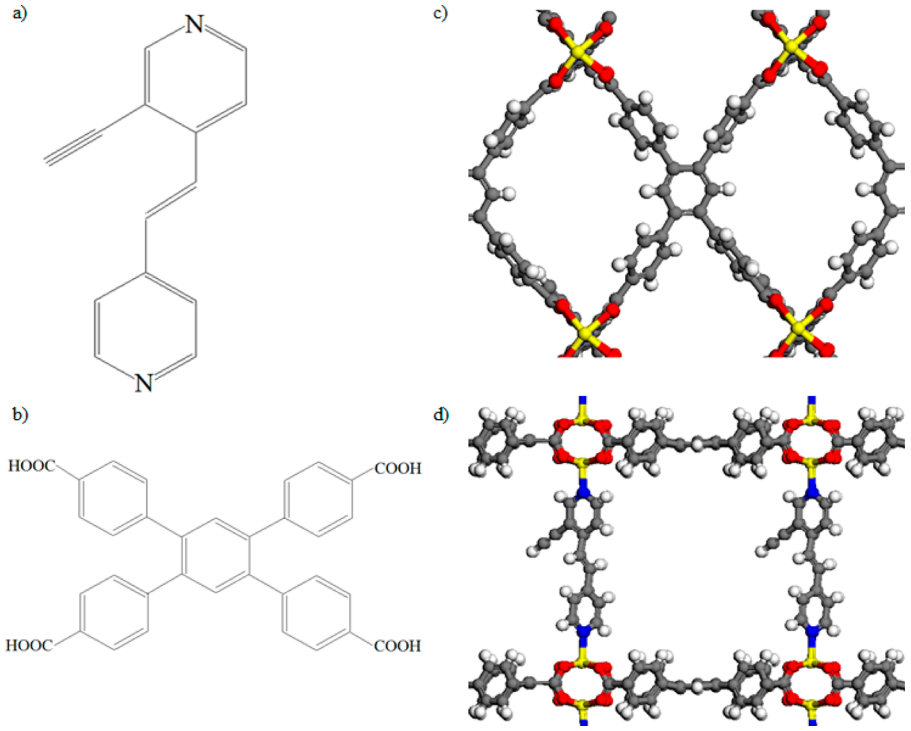

Figure 1. Organic ligands of DTO MOF: L1 (a) and TCPB (b). Two views of the DTO MOF structure (c) and (d). Gray, white, blue, red, and yellow colors represent carbon, hydrogen, nitrogen, oxygen, and zinc, respectively.

2. PROPOSED SYNTHESIS OF EXPOSED METAL SITES

The proposed postsynthesis modification of DTO is shown in Figure 2 using a smaller mimic of the acetylene-bearing DTO

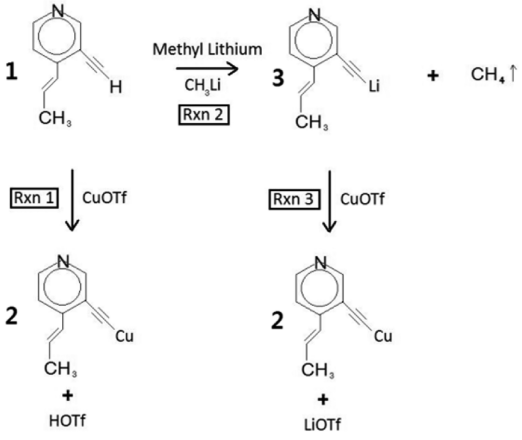

Figure 2. Two proposed reaction routes for Cu modification of an acetylene-bearing MOF linker to create highly exposed metal cations. Note that **1** is a smaller mimic of the MOF linker L1 and was used for computational ease.

linker. The objective is to replace the H atom at the terminus of the acetylene group with a monovalent cation, such as Cu^+ or Ag^+. Two routes are proposed. They are described here for copper, but incorporation of silver should follow a similar process. In the first route, the DTO MOF linker, **1**, reacts with copper(I) trifluoromethanesulfonate (CuOTf) to form **2** and trifluoromethanesulfonic acid (HOTf) via reaction 1. In the second possible route, **1** reacts with methyllithium (CH_3Li) (reaction 2) to form an intermediate, **3**, releasing methane. Then, **3** reacts with CuOTf to form **2** and LiOTf (reaction 3).

The thermodynamic feasibility of the proposed postsynthesis reactions was analyzed using quantum chemical methods. In addition, we computationally examined the binding properties of propylene and propane molecules with the created open metal sites and investigated the effect of solvent or LiOTf molecules, which might remain in the pores, on the binding of propylene and propane with the Cu or Ag sites.

3. COMPUTATIONAL METHODS

The reactions in Figure 2 and the binding of propane and propylene were investigated using the linker mimics shown in Figure 2. Geometry optimizations and total energy calculations of the various species were performed using the Gaussian09 software.[47] All calculations were performed with a hybrid basis set using 6-311+G(d,p) for all atoms except Cu and Ag, which were treated with the LANL2DZ basis set.[48−51] LANL2DZ is a well-established basis set for Cu and Ag, and 6-311G is compatible with LANL2DZ. These basis sets have been used before for complexes including Cu or Ag atoms.[52−55]

The binding energies, BE, of molecules with the Cu or Ag cluster models were calculated by

$$\mathrm{BE} = E(\text{linker} + \text{adsorbate}) - E(\text{linker}) - E(\text{adsorbate}) \quad (1)$$

where E is the total electronic energy. Counterpoise corrections were applied to E(linker + adsorbate) to offset basis set superposition errors (BSSE).[56−58] Additionally, natural bond orbital (NBO) analysis was performed to obtain insights into the changes of the electron populations in the orbitals of the Cu and Ag ions and the adsorbate molecules before and after the binding of propylene or propane.

Clusters were optimized at the B3LYP level of density functional theory (DFT) followed by total energy, single-point calculations at the MP2 level of theory. The MP2 method is generally more accurate for BE calculations than B3LYP, which

dx.doi.org/10.1021/jp502137j | J. Phys. Chem. C 2014, 118, 9086−9092

does not accurately describe dispersive interactions.[59,60] However, performing geometry optimizations of large clusters at the MP2 level of theory is computationally time-consuming, and DFT usually provides excellent predictions of geometries.

4. RESULTS AND DISCUSSION

Before examining possible reaction routes to replace the H atom at the terminus of the acetylene group on the linker with a monovalent cation, such as Cu^+ or Ag^+, we first calculated the preferred geometries of the product **2**. We considered 19 physically reasonable initial positions for the metal atom and performed geometry optimizations of the clusters using DFT. The initial metal positions included the position of the original hydrogen atom, 9 different positions around the C−C triple bond, and 9 different positions around the C−C double bond. Figure 3 shows the lowest energy positions of the Cu and Ag

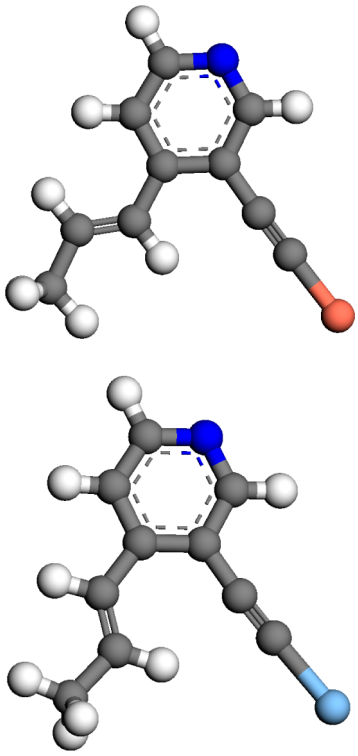

Figure 3. Lowest energy positions of Cu (top) and Ag (bottom) in the modified linkers. Gray, white, blue, brown, and light blue colors represent carbon, hydrogen, nitrogen, copper, and silver, respectively.

cations in the modified linkers. As we hoped, the metal cations adopt positions at the terminus of the acetylene group, with C−metal bond lengths of 1.83 and 2.04 Å for Cu and Ag, respectively. The longer bond length of Ag compared with Cu is understood from the larger van der Waals radius of the Ag atom (1.72 Å) compared to Cu atom (1.4 Å).[61] The C−C bond lengths (1.22−1.23 Å) were slightly elongated after metal incorporation, compared to the initial value (1.20 Å), but the C−C−metal bond angles remained at 180°, indicating that the triple-bond nature of the C−C bond was retained. In the case of the Cu-modified linker, our examination also produced another low-energy position where the metal atom was placed between the double bond and the triple bond of the linker. This position had an electronic energy 31−45 kJ/mol higher than the lowest energy position.

Next, we calculated the reaction energies for the three reactions shown in Figure 2 for both Cu and Ag. From the results in Table 1, it is clear that, for both metals, the first route

Table 1. Reaction Energies in kJ/mol for the Postsynthesis Modifications Proposed in Figure 2[a]

	reaction			
	1	2	3	2 + 3
Cu	59	−144	−166	−310
Ag	81	−143	−145	−288

[a]The energies were calculated by the B3LYP method.

(reaction 1) is highly endothermic and thus infeasible, but the second route (reaction 2 + reaction 3) is highly favorable thermodynamically. (Note that adding corrections for finite temperature will not change the qualitative conclusion.[62]) The production of free CH_4, a highly stable molecule, in the second route certainly plays a main role in the favorable thermodynamics. Humphrey and co-workers recently used postsynthesis modification of PCM-10, a porous phosphine coordination material based on Ca(II) and tris(*p*-carboxylated)-triphenylphosphine, to create exposed Au(I) sites.[63] They reported that the addition of AuCl onto the free P(III) Lewis base sites in PCM-10 created strong binding between the Au(I) Lewis acid and the P(III) Lewis base, yielding Au-PCM-10, a porous phosphine coordination material with open metal sites. This postsynthesis modification has some similarity with our proposal, although the sites proposed here are more highly unsaturated due to the release of LiOTf in our proposed scheme versus the retention of the chloride anion in the work of Humphrey and co-workers. The successful synthesis of Au-PCM-10 provides some indirect support for the feasibility of our proposed synthetic scheme.

After finding a plausible route for the incorporation of Cu^+ and Ag^+ sites on the linker, we examined the binding of propylene and propane molecules with the modified linkers. The optimized clusters for propane and propylene bound to the Cu- and Ag-modified linkers are illustrated in Figure 4. The calculated binding energies with B3LYP and MP2 are listed in Table 2 (first row and fourth row). As expected, both metals bind propylene more strongly than propane. In addition, the hydrocarbons adsorb more strongly on the Cu sites than the Ag sites. Cu binds propylene through a strong π complexation between the metal atom and the C−C double bond, with Cu−C distances of 2.08 and 2.14 Å. In the case of propane, Cu interacts with only one carbon atom based on binding distances of 2.24 and 3.38 Å. The longer distances for propane are consistent with a weaker interaction. The Ag modified linker exhibits similar behavior, with binding distances of 2.38 and 2.46 Å for propylene. As above, the larger van der Waals radius of Ag compared to Cu is responsible for the longer binding distances.

Humphrey and co-workers reported that Au-PCM-10 containing Au(I) sites in a similar environment to those examined here had much higher uptake of 1-hexene than *n*-hexane due to strong π complexation between the metal and the C−C double bond.[63] Jiang et al. employed DFT calculations to predict the binding energy of propylene with a silica-supported silver salt, which was generated by replacing one proton of a surface hydroxyl group with Ag^+.[64] They reported a binding energy of −69.5 kJ/mol, which is comparable to our results for propylene and the Ag-modified

dx.doi.org/10.1021/jp502137j | J. Phys. Chem. C 2014, 118, 9086−9092

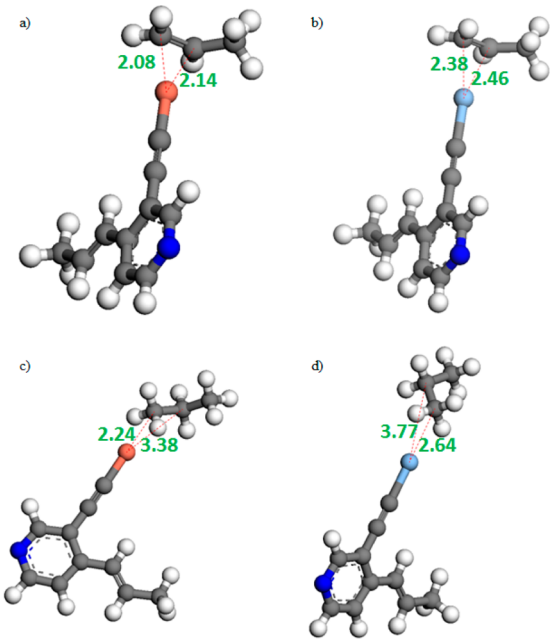

Figure 4. Optimized positions for propylene (top) and propane (bottom) interacting with Cu (left) and Ag (right) modified linkers. Gray, white, blue, brown, and light blue colors represent carbon, hydrogen, nitrogen, copper, and silver, respectively. The green values represent binding distances in Å between metal and carbon atoms.

Table 2. Calculated Binding Energies (in kJ/mol) for Propylene and Propane with Cu- or Ag-Modified Linkers with and without LiOTf (Side Product) or Diethyl Ether (Solvent)

	propylene		propane	
	B3LYP	MP2	B3LYP	MP2
Cu	−119	−140	−50.4	−58.4
Cu + LiOTf	−46.3	−60.2	−0.55	−1.49
Cu + diethyl ether	−4.68	−12.5	−0.46	−5.60
Ag	−78.0	−71.6	−25.4	−20.7
Ag + LiOTf	−44.1	−42.6	−5.45	−7.47
Ag + diethyl ether	−4.84	−14.0	−0.10	−5.39

linker. Chen and Yang used extended Hückel molecular orbital (EHMO) calculations to examine the binding energies of propylene with Cu^+- and Ag^+-exchanged sulfonic acid resins, in which exposed metal cations were created by substituting the proton of the sulfonic acid.[66] They reported propylene binding energies of −204.6 and −107.1 kJ/mol, respectively.[66] These energies are larger in magnitude than those in Table 2, but the trend between metals is similar. Note that the EHMO method is not as accurate as the methods used here, and thus, in addition to differences in the systems examined, different levels of theory might also contribute to differences in the binding energies. Lamia et al. reported an experimental isosteric heat of adsorption (Q_{st}) for propylene in HKUST-1 with open Cu^{2+} sites in the range of 40−50 kJ/mol,[33] and Yoon et al. reported an experimental Q_{st} for propylene in MIL-100(Fe) close to 70 kJ/mol,[35] both obtained at low loadings. These results suggest that the modified DTO linkers have lower propylene affinity than the exchanged sulfonic acid resins but stronger affinity than HKUST-1 and MIL-100 MOFs. For propane, our calculated binding energies with the Cu-modified linker are higher than those reported by Lamia et al.[33] (ca. 30 kJ/mol) but similar to the ones reported by Chen and Yang[66] (−55.6 kJ/mol).

We further studied the interactions of propylene with the Cu and Ag linkers using NBO analysis. The electron population changes upon adsorption of propylene for the Cu and Ag orbitals, as well as for the π orbital associated with the C−C double bond, are given in Table 3. The NBO analysis

Table 3. NBO Analysis of Propylene Adsorbed on a Cu- or Ag-Modified Linker[a]

orbital	Cu	Ag
s (Me)	0.161	0.170
p (Me)	0.083	0.051
d (Me)	−0.078	−0.070
$\sum$(s + p) (Me)	0.244	0.221
π-C−C double bond	−0.104	−0.089

[a]Shown are the changes in the electron populations of selected Cu and Ag orbitals (Me), as well as the π orbital of propylene, upon the adsorption of propylene.

demonstrates strong π complexation between the metal atoms and the propylene double bond. Donation of electrons from the π orbital of propylene leads to an increase in the population of the s and p orbitals of the metal atoms, while back-donation of electrons from the metal d orbitals to the antibonding π^* orbital of propylene gives rise to a decrease in the population of the metal orbitals. The net decrease in the population of the π orbital of propylene leads to an increase in the bond length of the propylene double bond from 1.33 to 1.37 Å for adsorption on Cu and 1.36 Å for adsorption on Ag. In addition, we were able to quantify the fundamentals of the stronger binding of propylene with Cu compared to Ag: the population change resulting from the electron donation from the C−C double bond to the s and p metal orbitals is higher for Cu (0.244) than for Ag (0.221), and the population change in the propylene π orbital is also higher in magnitude for Cu (−0.104) than for Ag (−0.089). Moreover, the back-donation from the metal d orbital is higher in the case of Cu than for Ag (−0.078 versus −0.070).

The results so far assume that the metal sites are fully accessible to guest molecules such as propane or propylene. However, in an experimental postsynthesis treatment based on Figure 2, it may be difficult to fully activate the material, and small amounts of solvent or reaction byproducts such as LiOTf may remain in the pores. Note that the pores of the DTO MOF are large enough for propylene or propane to be adsorbed on the open metal sites even in the presence of the impurities (e.g., solvents or LiOTf). These molecules may compete with the desired molecules (i.e., propylene) on the open metal adsorption sites. To assess the effect of this possibility, we calculated the binding energies of propane and propylene in the presence of a typical solvent, diethyl ether (DEE) or LiOTf, as defined by

$$\mathrm{BE} = E(\text{linker–impurity} + \text{adsorbate}) - E(\text{linker–impurity}) - E(\text{adsorbate}) \quad (2)$$

where "impurity" is either DEE or LiOTf and "adsorbate" is either propane or propylene. The linker−impurity + adsorbate cluster was obtained by a geometry optimization of a linker−impurity cluster followed by the addition of the adsorbate in different initial positions for further geometry optimization.

dx.doi.org/10.1021/jp502137j | J. Phys. Chem. C 2014, 118, 9086−9092

The optimized clusters are shown in Figure 5 for LiOTf, and the binding energies are given in Table 2. Interestingly, the Li

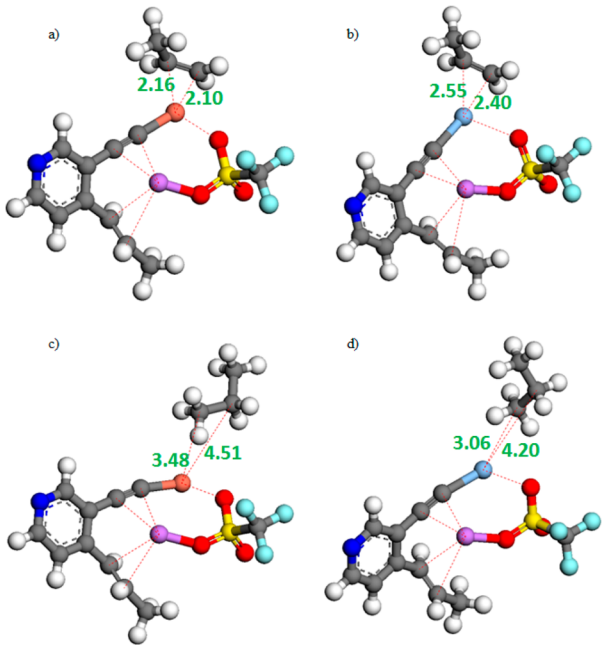

Figure 5. Optimized positions for propylene (top) and propane (bottom) adsorbed on Cu (left) and Ag (right) modified linkers including the LiOTf byproduct. Gray, white, blue, brown, light blue, violet, red, cyan, and yellow colors represent carbon, hydrogen, nitrogen, copper, silver, lithium, oxygen, fluorine, and sulfur, respectively. The green values represent binding distances in Å between linkers and hydrocarbons.

cations are located, in all cases, between the C−C double and triple bonds of the linker. In the case of propane, the bending of the C−C−Cu and C−C−Ag bonds of the linker indicates that the C−C triple-bond nature is not retained due to sharing of electrons between the π orbitals and the Li cation. The C−C bond lengths in the C−C−Cu and C−C−Ag bonds were slightly elongated by 0.01 Å. However, a more important feature is that one of the oxygen atoms from LiOTf bonds with the Cu or Ag atom, decreasing its propensity to interact with other molecules such as propylene. This is reflected in the sharply reduced binding energies in Table 2. The binding energies of propane drop to less than 10 kJ/mol in magnitude, but the binding energy of propylene is still fairly high, suggesting that the metal sites might be useful for propane/propylene separations even in the presence of LiOTf.

Similarly, we considered the presence of the diethyl ether solvent. The optimized clusters are shown in Figure 6, and the binding energies are given in Table 2. Again, the binding energies are sharply reduced in the presence of DEE. Remarkably, the decrease in the Cu−propylene binding energy is much sharper than in the presence of LiOTf, resulting in a binding energy reduction of 91% at the MP2 level of theory. This could be due to the existence of a steric effect, where bulky DEE molecules impede the approach of propylene molecules to the open metal sites, a situation that does not arise in the case of LiOTf due to the highly localized siting of the Li cation between the C−C double and triple bonds of the linker. Thus, the binding distances between linkers and hydrocarbons in the case of DEE are longer than in the case of LiOTf. All of these factors indicate that the interaction of the Cu and Ag linker

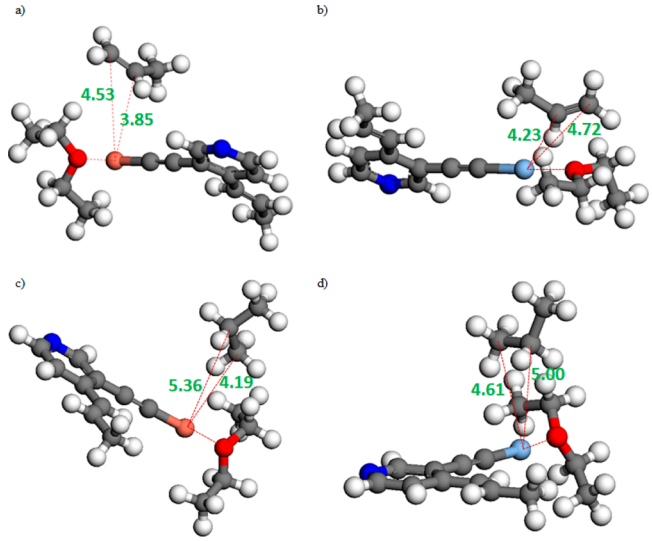

Figure 6. Optimized positions for propylene (top) and propane (bottom) adsorbed on Cu (left) and Ag (right) modified linkers including DEE solvent. Gray, white, blue, brown, light blue, and red colors represent carbon, hydrogen, nitrogen, copper, silver, and oxygen, respectively. The green values represent binding distances in Å between linkers and hydrocarbons.

atoms with the electron-rich O atom of the DEE solvent molecules is stronger than the π complexation between the metal and propylene.

The effect of LiOTf or DEE, which may potentially remain in the pores, demonstrates that these molecules will compete with the adsorption of propylene and propane on the open metal sites. However, it is important to note that even if the presence of LiOTf impedes the binding of open Cu and Ag sites with propane, they still bind propylene strongly. The prediction that propylene is still strongly adsorbed on the modified linkers while propane is hardly adsorbed suggests that these systems may be promising for propylene/propane separation.

5. CONCLUSIONS

We have studied the thermodynamic feasibility of incorporating highly unsaturated, monovalent Cu and Ag sites into the metal−organic framework DTO in a postsynthesis procedure. Quantum chemical calculations suggest that a two-step reaction sequence proposed here is thermodynamically favorable to create accessible Cu and Ag sites within the linker of the DTO MOF and that these sites show a strong preferential binding of propylene compared to propane. An NBO analysis illustrated that propylene forms stronger π complexation interactions with Cu than Ag, in line with the calculated binding energies. The results suggest that the Cu^+ and Ag^+ sites may also be useful for separating other paraffin/olefin pairs, such as ethane and ethylene. We also studied the effect of LiOTf, a byproduct of the postsynthesis modification, and DEE, a typical solvent, on the binding energies of propylene and propane with the open metal sites. The results showed that the presence of DEE sharply reduces the binding energies of both propylene and propane with the metal sites. On the other hand, the presence of LiOTf yielded extremely weak interactions between the open metal sites and propane but still strong interactions with propylene. This indicates that competition among these molecules for the metal adsorption sites might not necessarily be harmful for mixture separations and could even be part of

dx.doi.org/10.1021/jp502137j | J. Phys. Chem. C 2014, 118, 9086−9092

the molecular engineering of future sorbents for propane/propylene and other challenging separations.

AUTHOR INFORMATION

Corresponding Author

*E-mail: snurr@northwestern.edu (R.Q.S.).

Notes

The authors declare the following competing financial interest(s): J.T.H. and R.Q.S. have a financial interest in the start-up company NuMat Technologies, which is seeking to commercialize metal−organic frameworks.

ACKNOWLEDGMENTS

We acknowledge the Defense Threat Reduction Agency (HDTRA1-10-1-0023) for financial support and XSEDE for computational resources on Steele at Purdue University under Project Number TG-CTS080002. D.F.-J. thanks the Royal Society for a University Research Fellowship.

REFERENCES

(1) Zhou, H.-C.; Long, J. R.; Yaghi, O. M. Introduction to Metal-Organic Frameworks. *Chem. Rev.* **2012**, *112* (2), 673−674.

(2) Rowsell, J.; Yaghi, O. M. Strategies for Hydrogen Storage in Metal-Organic Frameworks. *Angew. Chem., Int. Ed.* **2005**, *44* (30), 4670−4679.

(3) Kaye, S. S.; Dailly, A.; Yaghi, O. M.; Long, J. R. Impact of Preparation and Handling on the Hydrogen Storage Properties of Zn_4O(1,4-benzenedicarboxylate)$_3$ (MOF-5). *J. Am. Chem. Soc.* **2007**, *129* (46), 14176−14177.

(4) Choi, H. J.; Dinca, M.; Long, J. R. Broadly Hysteretic H_2 Adsorption in the Microporous Metal-Organic Framework Co(1,4-Benzenedipyrazolate). *J. Am. Chem. Soc.* **2008**, *130* (25), 7848−7850.

(5) Zhou, W.; Yildirim, T. Nature and Tunability of Enhanced Hydrogen Binding in Metal-Organic Frameworks with Exposed Transition Metal Sites. *J. Phys. Chem. C* **2008**, *112* (22), 8132−8135.

(6) Furukawa, H.; Yaghi, O. M. Storage of Hydrogen, Methane, and Carbon Dioxide in Highly Porous Covalent Organic Frameworks for Clean Energy Applications. *J. Am. Chem. Soc.* **2009**, *131* (25), 8875−8883.

(7) Tan, C.; Yang, S.; Champness, N. R.; Lin, X.; Blake, A. J.; Lewis, W.; Schröder, M. High Capacity Gas Storage by a 4,8-Connected Metal-Organic Polyhedral Framework. *Chem. Commun.* **2011**, *47* (15), 4487−4489.

(8) Han, S. S.; Choi, S.-H.; Goddard, W. A., III Improved H_2 Storage in Zeolitic Imidazolate Frameworks Using Li^+, Na^+, and K^+ Dopants, with an Emphasis on Delivery H_2 Uptake. *J. Phys. Chem. C* **2011**, *115* (8), 3507−3512.

(9) Makal, T. A.; Li, J.-R.; Lu, W.; Zhou, H.-C. Methane Storage in Advanced Porous Materials. *Chem. Soc. Rev.* **2012**, *41* (23), 7761−7779.

(10) Demessence, A.; Long, J. R. Selective Gas Adsorption in the Flexible Metal-Organic Frameworks Cu(BDTri)L (L = DMF, DEF). *Chem.—Eur. J.* **2010**, *16* (20), 5902−5908.

(11) Herm, Z. R.; Krishna, R.; Long, J. R. CO_2/CH_4, CH_4/H_2 and $CO_2/CH_4/H_2$ Separations at High Pressures Using Mg_2(DOBDC). *Microporous Mesoporous Mater.* **2012**, *151*, 481−487.

(12) Bae, Y.-S.; Mulfort, K. L.; Frost, H.; Ryan, P.; Punnathanam, S.; Broadbelt, L. J.; Hupp, J. T.; Snurr, R. Q. Separation of CO_2 from CH_4 Using Mixed-Ligand Metal-Organic Frameworks. *Langmuir* **2008**, *24* (16), 8592−8598.

(13) Bao, Z.; Yu, L.; Ren, Q.; Lu, X.; Deng, S. Adsorption of CO_2 and CH_4 on a Magnesium-Based Metal Organic Framework. *J. Colloid Interface Sci.* **2011**, *353* (2), 549−556.

(14) Bastin, L.; Barcia, P. S.; Hurtado, E. J.; Silva, J. A. C.; Rodrigues, A. E.; Chen, B. A Microporous Metal-Organic Framework for Separation of CO_2/N_2 and CO_2/CH_4 by Fixed-Bed Adsorption. *J. Phys. Chem. C* **2008**, *112* (5), 1575−1581.

(15) Inubushi, Y.; Horike, S.; Fukushima, T.; Akiyama, G.; Matsuda, R.; Kitagawa, S. Modification of Flexible Part in Cu^{2+} Interdigitated Framework for CH_4/CO_2 Separation. *Chem. Commun.* **2010**, *46* (48), 9229−9231.

(16) Pianwanit, A.; Kritayakornupong, C.; Vongachariya, A.; Selphusit, N.; Ploymeerusmee, T.; Remsungnen, T.; Nuntasri, D.; Fritzsche, S.; Hannongbua, S. The Optimal Binding Sites of CH_4 and CO_2 Molecules on the Metal-Organic Framework MOF-5: ONIOM Calculations. *Chem. Phys.* **2008**, *349* (1−3), 77−82.

(17) Yang, Q.; Ma, L.; Zhong, C.; An, X.; Liu, D. Enhancement of CO_2/N_2 Mixture Separation Using the Thermodynamic Stepped Behavior of Adsorption in Metal-Organic Frameworks. *J. Phys. Chem. C* **2011**, *115* (6), 2790−2797.

(18) Krishna, R.; van Baten, J. M. Comment on Comparative Molecular Simulation Study of CO_2/N_2 and CH_4/N_2 Separation in Zeolites and Metal-Organic Frameworks. *Langmuir* **2010**, *26* (4), 2975−2978.

(19) Yang, Q.; Xu, Q.; Liu, B.; Zhong, C.; Smit, B. Molecular Simulation of CO_2/H_2 Mixture Separation in Metal-Organic Frameworks: Effect of Catenation and Electrostatic Interactions. *Chin. J. Chem. Eng.* **2009**, *17* (5), 781−790.

(20) Yuan, B.; Ma, D.; Wang, X.; Li, Z.; Li, Y.; Liu, H.; He, D. A Microporous, Moisture-Stable, and Amine-Functionalized Metal-Organic Framework for Highly Selective Separation of CO_2 from CH_4. *Chem. Commun.* **2012**, *48* (8), 1135−1137.

(21) Li, J.-R.; Sculley, J.; Zhou, H.-C. Metal-Organic Frameworks for Separations. *Chem. Rev.* **2012**, *112* (2), 869−932.

(22) Yang, Q.; Liu, D.; Zhong, C.; Li, J.-R. Development of Computational Methodologies for Metal-Organic Frameworks and Their Application in Gas Separations. *Chem. Rev.* **2013**, *113* (10), 8261−8323.

(23) Lee, J.; Farha, O. K.; Roberts, J.; Scheidt, K. A.; Nguyen, S. T.; Hupp, J. T. Metal-Organic Framework Materials as Catalysts. *Chem. Soc. Rev.* **2009**, *38*, 1450−1459.

(24) Xie, Z.; Wang, C.; deKrafft, K. E.; Lin, W. Highly Stable and Porous Cross-Linked Polymers for Efficient Photocatalysis. *J. Am. Chem. Soc.* **2011**, *133* (7), 2056−2059.

(25) Dang, D.; Wu, P.; He, C.; Xie, Z.; Duan, C. Homochiral Metal-Organic Frameworks for Heterogeneous Asymmetric Catalysis. *J. Am. Chem. Soc.* **2010**, *132* (41), 14321−14323.

(26) Alkordi, M. H.; Liu, Y.; Larsen, R. W.; Eubank, J. F.; Eddaoudi, M. Zeolite-Like Metal-Organic Frameworks as Platforms for Applications: On Metalloporphyrin-Based Catalysts. *J. Am. Chem. Soc.* **2008**, *130* (38), 12639−12641.

(27) Greathouse, J. A.; Ockwig, N. W.; Criscenti, L. J.; Guilinger, T. R.; Pohl, P.; Allendorf, M. D. Computational Screening of Metal-Organic Frameworks for Large-Molecule Chemical Sensing. *Phys. Chem. Chem. Phys.* **2010**, *12* (39), 12621−12629.

(28) Allendorf, M. D.; Houk, R. J. T.; Andruszkiewicz, L.; Talin, A. A.; Pikarsky, J.; Choudhury, A.; Gall, K. A.; Hesketh, P. J. Stress-Induced Chemical Detection Using Flexible Metal−Organic Frameworks. *J. Am. Chem. Soc.* **2008**, *130* (44), 14404−14405.

(29) Lan, A.; Li, K. W.; Haohan; Olson, D. H. E.; Thomas, J.; Ki, W.; Hong, M.; Li, J. A Luminescent Microporous Metal-Organic Framework for the Fast and Reversible Detection of High Explosives. *Angew. Chem., Int. Ed.* **2009**, *48* (13), 2334−2338.

(30) Ni, Z.; Jerrell, J. P.; Cadwallader, K. R.; Masel, R. I. Metal-Organic Frameworks as Adsorbents for Trapping and Preconcentration of Organic Phosphonates. *Anal. Chem.* **2007**, *79* (4), 1290−1293.

(31) Kreno, L. E.; Leong, K.; Farha, O. K.; Allendorf, M. D.; Van Duyne, R. P.; Hupp, J. T. Metal−Organic Framework Materials as Chemical Sensors. *Chem. Rev.* **2012**, *112* (2), 1105−1125.

(32) Kreno, L. E.; Hupp, J. T.; Van Duyne, R. P. Metal-Organic Framework Thin Film for Enhanced Localized Surface Plasmon Resonance Gas Sensing. *Anal. Chem.* **2010**, *82* (19), 8042−8046.

(33) Lamia, N.; Jorge, M.; Granato, M. A.; Almeida Paz, F. A.; Chevreau, H.; Rodrigues, A. E. Adsorption of Propane, Propylene and Isobutane on a Metal-Organic Framework: Molecular Simulation And Experiment. *Chem. Eng. Sci.* **2009**, *64* (14), 3246−3259.

(34) Ferreira, A. F. P.; Santos, J. C.; Plaza, M. G.; Lamia, N.; Loureiro, J. M.; Rodrigues, A. E. Suitability of Cu-BTC Extrudates for Propane-Propylene Separation by Adsorption Processes. *Chem. Eng. J.* **2011**, *167* (1), 1−12.
(35) Yoon, J. W.; Seo, Y.-K.; Hwang, Y. K.; Chang, J.-S.; Leclerc, H.; Wuttke, S.; Bazin, P.; Vimont, A.; Daturi, M.; Bloch, E.; Llewellyn, P. L.; Serre, C.; Horcajada, P.; Greneche, J.-M.; Rodrigues, A. E.; Ferey, G. Controlled Reducibility of a Metal-Organic Framework with Coordinatively Unsaturated Sites for Preferential Gas Sorption. *Angew. Chem., Int. Ed.* **2010**, *49* (34), 5949−5952.
(36) Jorge, M.; Lamia, N.; Rodrigues, A. E. Molecular Simulation of Propane/Propylene Separation on the Metal-Organic Framework CuBTC. *Colloids Surf., A* **2010**, *357* (1−3), 27−34.
(37) Lee, C. Y.; Bae, Y.-S.; Jeong, N. C.; Farha, O. K.; Sarjeant, A. A.; Stern, C. L.; Nickias, P.; Snurr, R. Q.; Hupp, J. T.; Nguyen, S. T. Kinetic Separation of Propene and Propane in Metal-Organic Frameworks: Controlling Diffusion Rates in Plate-Shaped Crystals via Tuning of Pore Apertures and Crystallite Aspect Ratios. *J. Am. Chem. Soc.* **2011**, *133* (14), 5228−5231.
(38) Bao, Z.; Alnemrat, S.; Yu, L.; Vasiliev, I.; Ren, Q.; Lu, X.; Deng, S. Adsorption of Ethane, Ethylene, Propane, and Propylene on a Magnesium-Based Metal-Organic Framework. *Langmuir* **2011**, *27* (22), 13554−13562.
(39) Uchida, S.; Eguchi, R.; Nakamura, S.; Ogasawara, Y.; Kurosawa, N.; Mizuno, N. Selective Sorption of Olefins by Halogen-Substituted Macrocation-Polyoxometalate Porous Ionic Crystals. *Chem. Mater.* **2012**, *24* (2), 325−330.
(40) Plaza, M. G.; Ribeiro, A. M.; Ferreira, A.; Santos, J. C.; Lee, U.-H.; Chang, J.-S.; Loureiro, J. M.; Rodrigues, A. E. Propylene/Propane Separation by Vacuum Swing Adsorption Using Cu-BTC Spheres. *Sep. Purif. Technol.* **2012**, *90*, 109−119.
(41) Fischer, M.; Gomes, J. R. B.; Froeba, M.; Jorge, M. Modeling Adsorption in Metal-Organic Frameworks with Open Metal Sites: Propane/Propylene Separations. *Langmuir* **2012**, *28* (22), 8537−8549.
(42) Plaza, M. G.; Ferreira, A. F. P.; Santos, J. C.; Ribeiro, A. M.; Mueller, U.; Trukhan, N.; Loureiro, J. M.; Rodrigues, A. E. Propane/Propylene Separation by Adsorption Using Shaped Copper Trimesate MOF. *Microporous Mesoporous Mater.* **2012**, *157*, 101−111.
(43) Bae, Y.-S.; Lee, C. Y.; Kim, K. C.; Farha, O. K.; Nickias, P.; Hupp, J. T.; Nguyen, S. T.; Snurr, R. Q. High Propene/Propane Selectivity in Isostructural Metal−Organic Frameworks with High Densities of Open Metal Sites. *Angew. Chem., Int. Ed.* **2012**, *51* (8), 1857−1860.
(44) Geier, S. J.; Mason, J. A.; Bloch, E. D.; Queen, W. L.; Hudson, M. R.; Brown, C. M.; Long, J. R. Selective Adsorption of Ethylene over Ethane and Propylene over Propane in the Metal−Organic Frameworks M_2(DOBDC) (M = Mg, Mn, Fe, Co, Ni, Zn). *Chem. Sci.* **2013**, *4*, 2054−2061.
(45) Bao, Z.; Alnemrat, S.; Yu, L.; Vasiliev, I.; Ren, Q.; Lu, X.; Deng, S. Adsorption of Ethane, Ethylene, Propane, and Propylene on a Magnesium-Based Metal−Organic Framework. *Langmuir* **2011**, *27* (22), 13554−13562.
(46) Bloch, E. D.; Queen, W. L.; Krishna, R.; Zadrozny, J. M.; Brown, C. M.; Long, J. R. Hydrocarbon Separations in a Metal-Organic Framework with Open Iron(II) Coordination Sites. *Science* **2012**, *335* (6076), 1606−1610.
(47) Frisch, M. J.; Trucks, G. W.; Schlegel, H. B.; Scuseria, G. E.; Robb, M. A.; Cheeseman, J. R.; Scalmani, G.; Barone, V.; Mennucci, B.; Petersson, G. A.; Nakatsuji, H.; Caricato, M.; Li, X.; Hratchian, H. P.; Izmaylov, A. F.; Bloino, J.; Zheng, G.; Sonnenberg, J. L.; Hada, M.; Ehara, M.; Toyota, K.; Fukuda, R.; Hasegawa, J.; Ishida, M.; Nakajima, T.; Honda, Y.; Kitao, O.; Nakai, H.; Vreven, T.; Montgomery, J. A., Jr.; Peralta, J. E.; Ogliaro, F.; Bearpark, M.; Heyd, J. J.; Brothers, E.; Kudin, K. N.; Staroverov, V. N.; Kobayashi, R.; Normand, J.; Raghavachari, K.; Rendell, A.; Burant, J. C.; Iyengar, S. S.; Tomasi, J.; Cossi, M.; Rega, N.; Millam, J. M.; Klene, M.; Knox, J. E.; Cross, J. B.; Bakken, V.; Adamo, C.; Jaramillo, J.; Gomperts, R.; Stratmann, R. E.; Yazyev, O.; Austin, A. J.; Cammi, R.; Pomelli, C.; Ochterski, J. W.; Martin, R. L.; Morokuma, K.; Zakrzewski, V. G.; Voth, G. A.; Salvador, P.; Dannenberg, J. J.; Dapprich, S.; Daniels, A. D.; Farkas, O.; Foresman, J. B.; Ortiz, J. V.; Cioslowski, J.; Fox, D. J. Gaussian 09, Revision A.02, Wallingford, CT, 2009.
(48) McLean, A. D.; Chandler, G. S. Contracted Gaussian Basis Sets for Molecular Calculations. I. Second Row Atoms, Z = 11−18. *J. Chem. Phys.* **1980**, *72* (10), 5639−5648.
(49) Hay, P. J.; Wadt, W. R. Ab Initio Effective Core Potentials for Molecular Calculations. Potentials for K to Au Including the Outermost Core Orbitals. *J. Chem. Phys.* **1985**, *82*, 299−310.
(50) Frisch, M. J.; Pople, J. A.; Binkley, J. S. Self-Consistent Molecular Orbital Methods. 25. Supplementary Functions for Gaussian Basis Sets. *J. Chem. Phys.* **1984**, *80*, 3265−3269.
(51) Krishnan, R.; Binkley, J. S.; Seeger, R.; Pople, J. A. Self-Consistent Molecular Orbital Methods. XX. A Basis Set for Correlated Wave Functions. *J. Chem. Phys.* **1980**, *72*, 650−654.
(52) Matulis, V. E.; Ivashkevich, O. A.; Gurin, V. S. DFT Study of Electronic Structure and Geometry of Neutral and Anionic Silver Clusters. *J. Mol. Struct.: THEOCHEM* **2003**, *664−665*, 291−308.
(53) Rios-Reyes, C. H.; Camacho-Mendoza, R. L.; Mendoza-Huizar, L. H. A Theoretical Quantum Study on the Distribution of Electrophilic and Nucleophilic Active Sites on Ag(100) Surfaces Modeled as Finite Clusters. *J. Mex. Chem. Soc.* **2006**, *50* (1), 19−27.
(54) Mori, S.; Nakamura, E. Correlation of Coordination Geometry of Copper Atom to Reactivities of Organocuprate. Molecular Orbital Analysis of Dimethylcuprate Anion. *Tetrahedron Lett.* **1999**, *40* (29), 5319−5322.
(55) Zhao, L.; Yang, Q.; Ma, Q.; Zhong, C.; Mi, J.; Liu, D. A Force Field for Dynamic Cu-BTC Metal-Organic Framework. *J. Mol. Model.* **2011**, *17* (2), 227−234.
(56) Daza, M. C.; Dobado, J. A.; Molina, J. M.; Salvador, P.; Duran, M.; Villaveces, J. L. Basis Set Superposition Error-Counterpoise Corrected Potential Energy Surfaces. Application to Hydrogen Peroxide...X (X = F^-, Cl^-, Br^-, Li^+, Na^+) Complexes. *J. Chem. Phys.* **1999**, *110* (24), 11806−11813.
(57) van Mourik, T.; Wilson, A. K.; Peterson, K. A.; Woon, D. E.; Dunning, T. H., Jr. The Effect of Basis Set Superposition Error (BSSE) on the Convergence of Molecular Properties Calculated with the Correlation Consistent Basis Sets. *Adv. Quantum Chem.* **1999**, *31*, 105−133.
(58) Boys, S. F.; Bernardi, F. The Calculation of Small Molecular Interactions by the Differences of Separate Total Energies. Some Procedures with Reduced Errors. *Mol. Phys.* **2002**, *100* (1), 65−73.
(59) Lee, C.; Yang, W.; Parr, R. G. Development of the Colle-Salvetti Correlation-Energy Formula into a Functional of the Electron Density. *Phys. Rev. B* **1988**, *37*, 785−789.
(60) Becke, A. D. Density-Functional Thermochemistry. III. The Role of Exact Exchange. *J. Chem. Phys.* **1993**, *98* (7), 5648−5652.
(61) Bondi, A. van der Waals Volumes and Radii. *J. Phys. Chem.* **1964**, *68* (3), 441−451.
(62) Alapati, S. V.; Johnson, J. K.; Sholl, D. S. Using First Principles Calculations to Identify New Destabilized Metal Hydride Reactions for Reversible Hydrogen Storage. *Phys. Chem. Chem. Phys.* **2007**, *9* (12), 1438−1452.
(63) Nunez, A. J.; Shear, L. N.; Dahal, N.; Ibarra, I. A.; Yoon, J.; Hwang, Y. K.; Chang, J.-S.; Humphrey, S. M. A Coordination Polymer of (Ph_3P)AuCl Prepared by Post-Synthetic Modification and Its Application in 1-Hexene/n-Hexane Separation. *Chem. Commun.* **2011**, *47*, 11855−11857.
(64) Jiang, D. E.; Sumpter, B. G.; Dai, S. Olefin Adsorption on Silica-Supported Silver Salts - A DFT Study. *Langmuir* **2006**, *22*, 5716−5722.
(65) Jiang, D. E.; Dai, S. Frst Principles Molecular Dynamics Simulation of A Task-Specific Ionic Liquid Based on Silver-Olefin Complex: Atomistic Insights into a Separation Process. *J. Phys. Chem. B* **2008**, *112*, 10202−10206.
(66) Chen, J. P.; Yang, R. T. A Molecular Orbital Study of the Selective Adsorption of Simple Hydrocarbon Molecules on Ag^+- and Cu^+-Exchanged Regins and Cuprous Halides. *Langmuir* **1995**, *11*, 3450−3456.